Late Quaternary regional geodynamics and hydraulic properties of the crystalline rocks of Fennoscandia

H. Henriksen *

Sogn og Fjordane University College, Faculty of Engineering and Science, Post box 133, 6851 Sogndal, Norway

Abstract

Hydraulic conductivity data derived from ca. 140, 000 crystalline rock boreholes from the upper 150 m of the crust of Norway and Sweden have been pre-processed in a GIS and subsequently subject to explorative data analysis and simple- and stepwise multiple linear regression methods. The variables that were evaluated include the annual postglacial uplift rate, lithology, soil thickness, relative relief, net precipitation and borehole depth. The results are discussed in light of the regional geodynamic framework especially that related to postglacial rebound and crustal deformation. The typical regional variables, the rate of postglacial uplift and net precipitation, explain only a small portion of the total variation in hydraulic conductivity. Drilled rock depth stands out as the most important predictor. Regional variations in hydraulic conductivity coincide with distinct irregularities in profile graphs of the uplift surface, suggesting an influence of recent geodynamics on hydraulic conductivity along localised zones of compression, tension and shear. It is believed that these findings, if further pursued, may contribute to the understanding of the complexity of the rebound tectonics associated with the late glacial and Holocene deglaciation.

Keywords: Crystalline rocks; Hydraulic conductivity; Postglacial rebound; Crustal deformation

1. Introduction

The hydraulic properties of crystalline rocks largely depend on the physical and geometrical properties of their fracture network (e.g. NRC, 1996). The capability of the fracture network to transmit water depends on fracture orientation, fracture frequency and physical fracture attributes like aperture, length and connectivity. The fracture network in hard rocks is the result of repeated brittle deformation episodes, each generating faults and fractures of different orientations and physical characteristics. Moreover, fractures with the greatest reactivation potential in the contemporary stress field tend to be the most water conducting (e.g. Barton et al., 1995), and unless reactivated, older fractures are in general less permeable than younger or recent fractures. This means that a dynamic understanding of the fracture pattern, and the stresses that caused the formation of the fractures in the rock body through time, is a necessity to deduce the hydrogeological importance of the individual fracture sets (e.g. Cohen, 1995; Henriksen and Braathen, 2006).

The Fennoscandian shield (Fig.1) is a cratonic area with a core of Archean and Early Proterozoic gneisses and greenstone belts that are exposed in Karelia, northwest Finland, the Kola Peninsula, and in Lapland. Towards the west progressively younger crustal units are exposed. The Svecokarelian province consists of metasupracrustal rocks and granites, which were formed and metamorphosed about 2000 - 1650 million years ago, fringed by the N-S trending Transscandinavian belt (1800-1650 million years) with predominantly undeformed granites and acid volcanics. The Sveconorwegian province forms the western margin of the shield area and contains Proterozoic rocks that date back to about 1750-1500 million years and were metamorphosed in the Sveconorwegian orogeny about 1250-900 million years ago (Kullerud et al., 1986). Isolated remains of Phanerozoic sedimentary rocks cover the shield area in the Oslo area in southeastern Norway, and in southeastern and central Sweden.

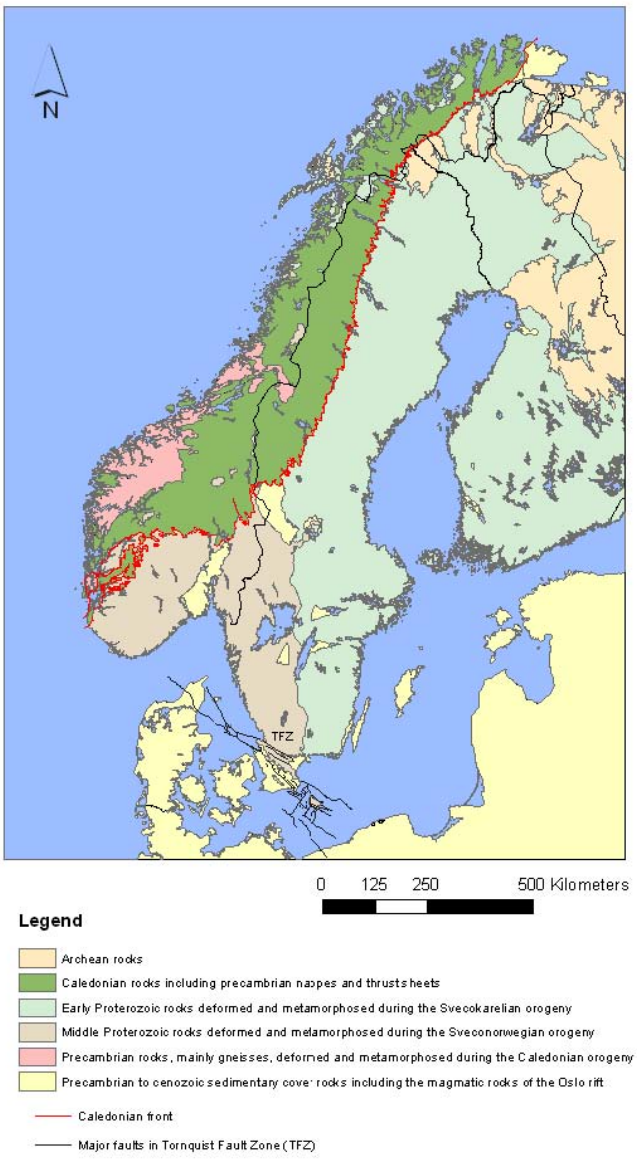

Fig.1.Geological map of Fennoscandia, modified from Sigmond (2002)

The 50 km broad Tornquist Fault Zone (Erlström et al., 1997), which extends NW-SE through Scania in South Sweden (Fig. 1), marks the border between the Fennoscandian shield and the sedimentary basin of continental Europe. South of this fault zone, there are sedimentary cover rocks of Cambrian to Tertiary age. During the Scandian phase of the Caledonian orogeny, about 400 million years ago (Milnes et al., 1997), a series of nappes containing oceanic fragments and basement rocks derived from the westernmost margin of Fennoscandia were emplaced southeastwards upon the shield along a 2000 km long and 100-200 km wide belt which extends from Stavanger in southwestern Norway to North Cape on the northern coast. The front of the Caledonian nappes extends into the western parts of central and northern Sweden.

Both crustal and lithosphere thicknesses show a considerable lateral variation (Babuska et al., 1988; Kinck et al., 1991). The thickest lithosphere (160-200 km) is in the Gulf of Bothnia, where

the thickness is about two to three times that of the coastal regions of Norway and southern Sweden. Crustal thickness shows a similar variation, but here the thickest crust (about 60 km) is found in Karelia in eastern Finland. The strongly asymmetric topography of Fennoscandia is dominated by two high domes, the northern Scandes and the southern Scandes, with a lower dome, the South Swedish dome, in

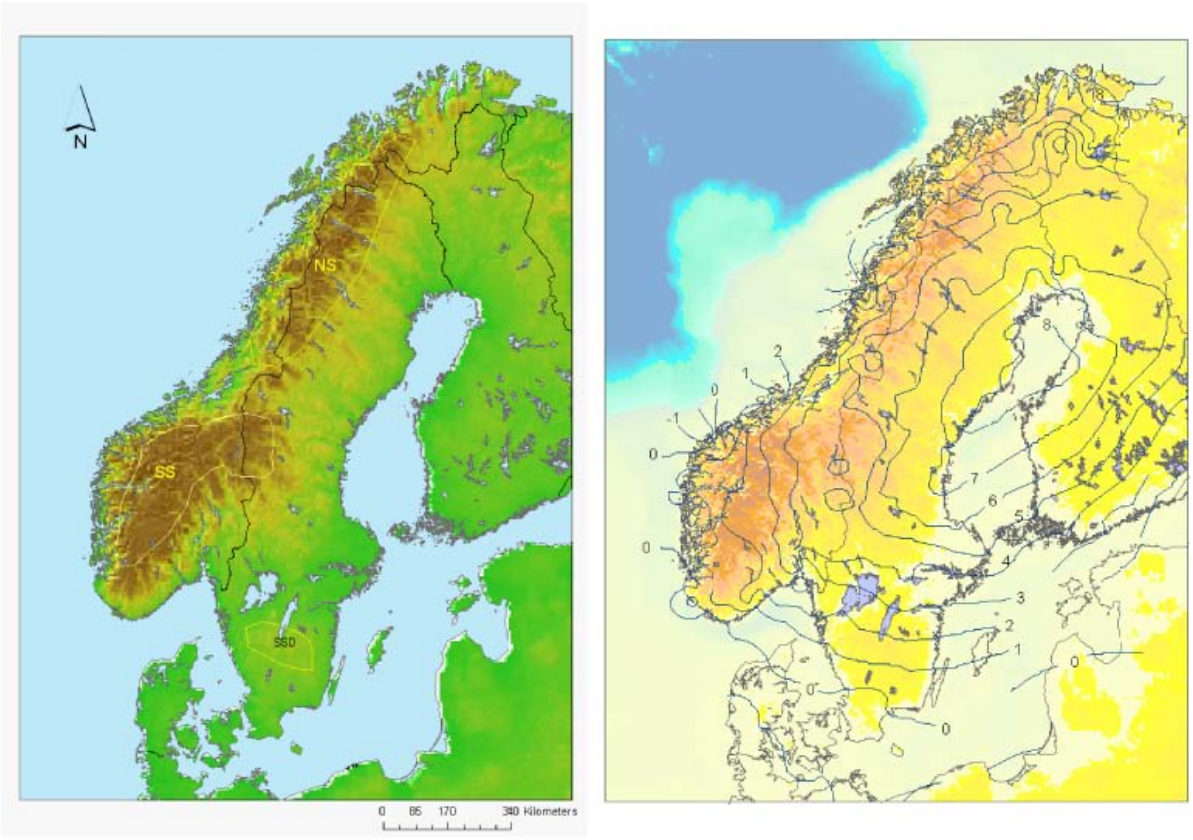

Fig.2. (a) Shaded relief map of Fennoscandia illustrating the main geomorphological features and (b) shaded relief map of Fennoscandia and ocean areas with isolines of annual uplift rate from the data of Dehls et al. (2000).

the south (Lidmar-Bergström, 1999; Fig. 2a). The highest relative relief, 1000-1500 m, is found in the western Scandes. Much of the eastern parts of Fennoscandia, including Sweden, has relative relief of less than 400 m. The present elevation and strongly asymmetric topography of Fennoscandia is a result of Neogene geodynamics (e.g. Faleide et al., 2002; Gabrielsen et al., 2005) and the highly contrasting relief features have been taken as indications of different vertical uplift of central and northern Fennoscandia by Paleogene and Miocene tectonism (Riis, 1996; Lidmar- Bergström, 1999).

The most recent crustal deformation in Fennoscandia is related to the still ongoing isostatic uplift of the lithosphere as a consequence of the downmelting of the Late Weichselian ice-sheet which had its maximum about 20,000 years ago. The history of the Late Weichselian glaciation and deglaciation has been dealt with in numerous works (e.g. Andersen, 1981; Lundqvist, 1986; Mangerud, 1991; Boulton et al., 2001). The vertical lithospheric uplift is well documented (Mörner, 1980; Ekman, 1996; Dehls et al., 2000) and can be pictured as a gradual return of the downwarped portion of the ice-loaded Fennoscandian crust back towards its original pre- ice age state. The crustal rebound (uplift) was initiated in the late glacial, about 7000 years before the region was completely deglaciated about 8500 BP (Mörner, 1979; Lambech et al., 1998). However, well-documented uplift data for the entire region are only available from the Holocene (postglacial) to recent. At the peak of the rebound, about 10,000 BP, absolute uplift rates were 50 -500 mm/year (Mörner, 1980). Ekman (1991) estimated the remaining uplift in the central parts to be about 50 m, while Fjeldskaar and Cathles (1991) suggested a remaining maximum uplift of 40 m. More recent simulations are in the range of 55-90 m (Kaufmann et al., 2000;

Ekman and Mäkinen, 1996). Hence, 90-95% of the total isostatic recovery, estimated to be 830 m, is now completed.

Generalised maps of the observed present rates of uplift are shown in Figs. 2b and 6. The maps are based on the uplift model for the 1:3 mill "Neotectonic Map of Norway and Adjacent Areas" (Dehls et al., 2000).The uplift model is based on data from tide-gauges (58), precise levellings (300), absolute gravity measurements (86) and permanent GPS stations (47) across the Fennoscandian region. This uplift model was also used by Fjeldskaar et al. (2000). More information about the model is found in Olesen et al. (2000), Dehls et al. (2000) and in the work of Fjeldskaar et al. (2000).

The region subjected to vertical uplift has an ellipsoidal shape with its long axis oriented SW-NE and with a central region of maximum uplift in the Gulf of Bothnia with a present uplift rate of about 9 mm/year (Ekman, 1996). Geologic mapping in the last decades have provided extensive records of recent and ongoing permanent crustal deformation which, alone or together with other stress sources, relate to the peak of rebound. They include seismotectonic features such as surface fracturing and faulting (e.g. Mörner, 2004; Olesen et al., 2004).

Models of glacial loading and unloading (e.g. Mitrovica et al., 1994; Wu et al., 1999) and continuous GPS monitoring of Fennoscandian crustal velocities (Milne et al., 2001, 2004) have thrown considerable light on the horizontal deformation field associated with the rebound. In short, the horizontal deformation is associated with crustal extension in the downwarped lithosphere and contraction in the adjacent forebulge. Horizontal crustal rates radiate, and increase with distance from the uplift centre and reach values of 1.5-2 mm/year at the margins of the former ice sheet (e.g. Mitrovica et al., 1994; Milne et al., 2001). From a hydrogeological point of view, it is the stresses associated with the horizontal component of the rebound that are of most interest because they have the greatest potential for affecting fracture apertures, reactivate fractures or initiate new fractures and faults. Modeling of the horizontal rebound stresses suggest that they, either alone or in combination with the ambient tectonic stresses, are able to reactivate existing fractures and faults or even initiate new brittle deformational structures in the uppermost crust. However, the nature, magnitude and orientation of these horizontal rebound stresses are predicted to vary both in space and time (Muir-Wood, 2000; Wu et al., 1999). Gudmundsson (1999) predicted a reverse and strike-slip stress regime in the marginal parts of the uplift region and a tensile, normal fault stress regime around the central part of the uplift dome.

The hydrogeological implications of the rebound stresses were addressed by Muir-Wood (1993 a, b) and later by Rohr-Torp (1994), Morland (1997) and Gudmundsson (1999). Both Rohr-Torp (1994) and Morland (1997) found a positive correlation between present uplift rates and yield of boreholes in crystalline rocks in Norway. They related their findings to a uniform postglacial rebound with gradually increasing horizontal tensile deformation, and increasing rock mass permeability, with increasing uplift rate. However, this relationship is not found if one considers the whole region of glacial rebound (Henriksen, 2003; Berggren, 1998). Two likely explanations for this discrepancy is that the uplift process is more complex than envisaged, or that other factors than glacial rebound stresses contribute to the regional variations in borehole flow rates.

Published maps of vertical and horizontal crustal rates, like those of Ekman (1996) and Milne et al. (2001), give only a smoothed and generalised first-order picture of these recent crustal motions. Abundant field evidence (e.g. Anundsen, 1989; Björkman and Trägårdh, 1982; Pan et al., 1999; Mörner, 1985, 2004; Talbot, 1992; Tirén and Beckholmen, 1989), detailed examination of geodetic re-levelling curves (Muir-Wood 1993a) and spatial distribution of intermediate wavelength components of a new uplift data set (Olesen et al., 2004) all indicate that differential movements are taking place between individual crustal blocks within the rebounding Fennoscandian lithosphere. A tectonic component related to a long-term Neogene uplift may also contribute to the observed present-day vertical deformation (Fjeldskaar et al., 2000).

The main objective of this paper is to investigate the spatial distribution of hydraulic conductivity values estimated from borehole flow rate data within a large part (about 600,000 km^2) of the

Fennoscandian region, and then relate this distribution not only to the recent geodynamics, but also to other factors that may influence the estimated values of the hydraulic conductivity.

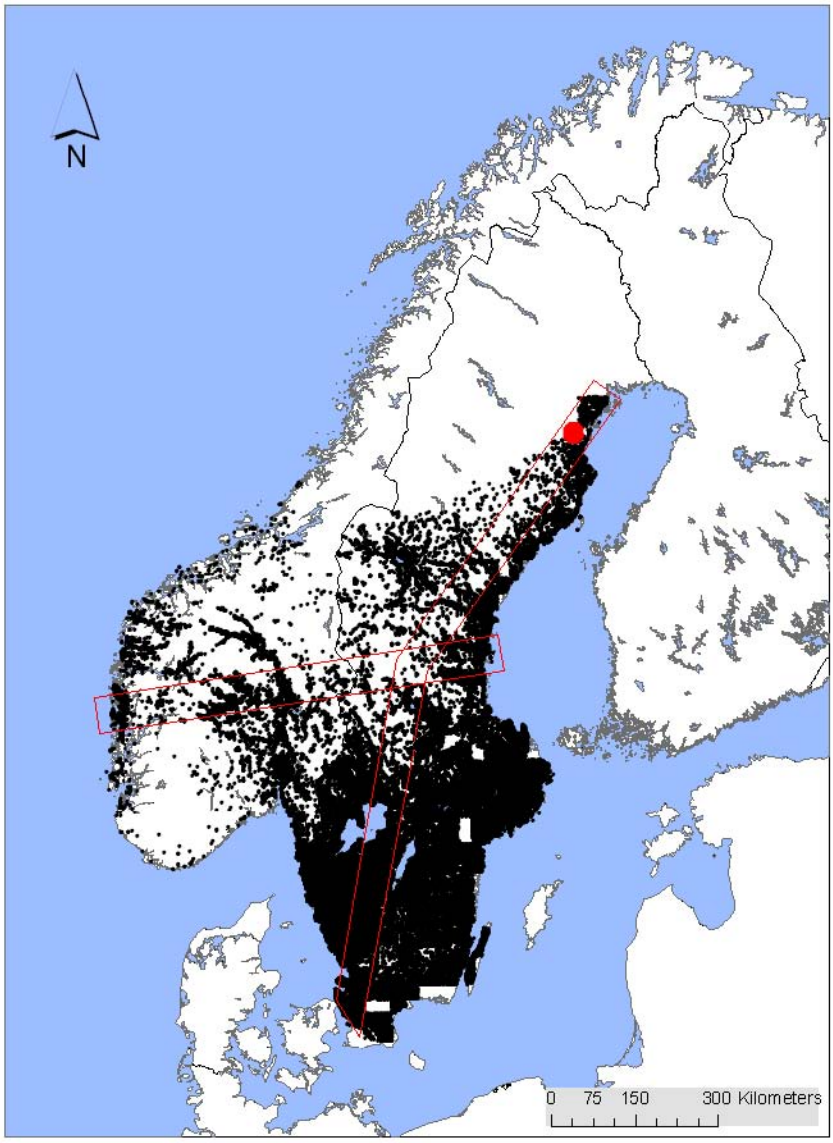

Fig. 3. Distribution of boreholes with flow rate data and estimates of hydraulic conductivty. The ″uplift centre″ in Ångermanland is indicated by a red symbol. Rectangles with red outline are profiles where subsets of borehole data have been analysed.

2. Estimation of hydraulic conductivity

The borehole data (Fig. 3) used to estimate the hydraulic conductivity were obtained from the databases of the Norwegian and Swedish Geological Surveys. The data set, initially about 165, 000 records, contain well site technical information such as well yield, well use, well diameter, well casing, well depth, depth to static water level and soil thickness. The bulk of well data are filed in by the drillers after completion of the well. These data may be of variable quality, and registration errors are likely. Quality-filtering techniques were applied to secure a reliable statistical analysis from the initially large volume of data. In order to eliminate wells possibly erroneously recorded as hard rock boreholes or wells whose flow rates are strongly influenced by the overlying soils, boreholes with total depths < 20 m or with a proportion of overburden ≥ 50% were deleted. Records with flow rate > 50 000 l/hr or with

flow rates < 100 l/hr were deleted to avoid boreholes in rocks with primary porosity, or wells with no entries for well discharge or with so small discharges that the capacities measured are highly inaccurate.

The bulk of the well data are from domestic wells. Flow rates *(Q)* are measured by air-blow flow tests performed by the driller during and at the termination of the drilling. Compressed air from the drill bit, placed at the bottom of the borehole, is used to blow the water out of the well. The flow rate of water in litres per hour is determined as the water exits the top of the well through a discharge pipe placed at the top of the well casing. Normally, the duration of an air-blow test is from 1 to 3 h.

Specific capacity (Singhal and Gupta, 1999) is the standard variable for comparing flow rates and productivities in crystalline rock aquifers. Its determination requires pumping tests of about 24 h duration at a constant rate, which are normally not performed in connection with the establishment of hard rock boreholes in Scandinavia. The normalised flow rate,

$$q = \frac{Q}{DRD} \tag{1}$$

where Q is the flow rate (m^3/s) and DRD (m) is the drilled rock depth (i.e. total well depth – soil thickness), is the most common estimate for hydraulic bedrock properties in the Scandinavian countries. It represents a conservative estimate of specific capacity and has been of great value in characterising the hydraulic properties of the Scandinavian hard rock environment (Rohr-Torp, 1994; Wallroth and Rosenbaum, 1995; Wladis and Gustafson, 1999; Morland, 1997; Henriksen, 2003).

Wladis and Gustafson (1999) compared transmissivity values from air blow data with transmissivity values from injection (packer) tests. They found that the log-transmissivity estimates from air blow data were within one order of magnitude compared to values from injection tests; and that their standard deviations were in close agreement.

Jetel (1964) and Jetel and Krásný (1968) introduced an index of hydraulic of conductivity defined by the parameter:

$$Z = \log(10^9 \cdot \frac{S_c}{h'}) \tag{2}$$

where h′ is the open section of the well in meter and S_c is the specific capacity expressed in m^2/s. This lognormally distributed parameter and a related index of transmissivity have been widely used in comparative regional studies of transmissivity and hydraulic conductivity of crystalline rocks (Krásný 1999). Carlsson and Carlstedt (1977) showed that the expression of Jetel and Krásný (1968), under non-steady state conditions, could be transformed to:

$$K = \frac{10^{(Z-9)}}{\alpha} \tag{3}$$

Here, *K* is the hydraulic conductivity (m/s) and α is a parameter that depends on well diameter, pumping time and hydraulic diffusivity. The value of α is in the range 0.9 – 1.1, but for most practical purposes its value can be taken as 1 (Berggren, 1998).

The records from the national well archives in most cases lack detailed pumping test data such as drawdown and duration of the pumping test. Hence, the actual drawdown was approximated by the

available drawdown, which was calculated as the difference between the total well depth and the static water level minus a fixed pump depth setting of 5 m above the bottom of the well (Fig. 4). Missing water level data, about 50% of the boreholes, were calculated as the overall mean of the water level data. The length of the open well section was calculated as the difference between the total well depth and the casing depth when the static water level was above the termination of the casing (Fig. 4a). When the static water level was lower than the casing depth, the length of the open section was calculated as the difference between the total well depth and the static water level (Fig. 4b).

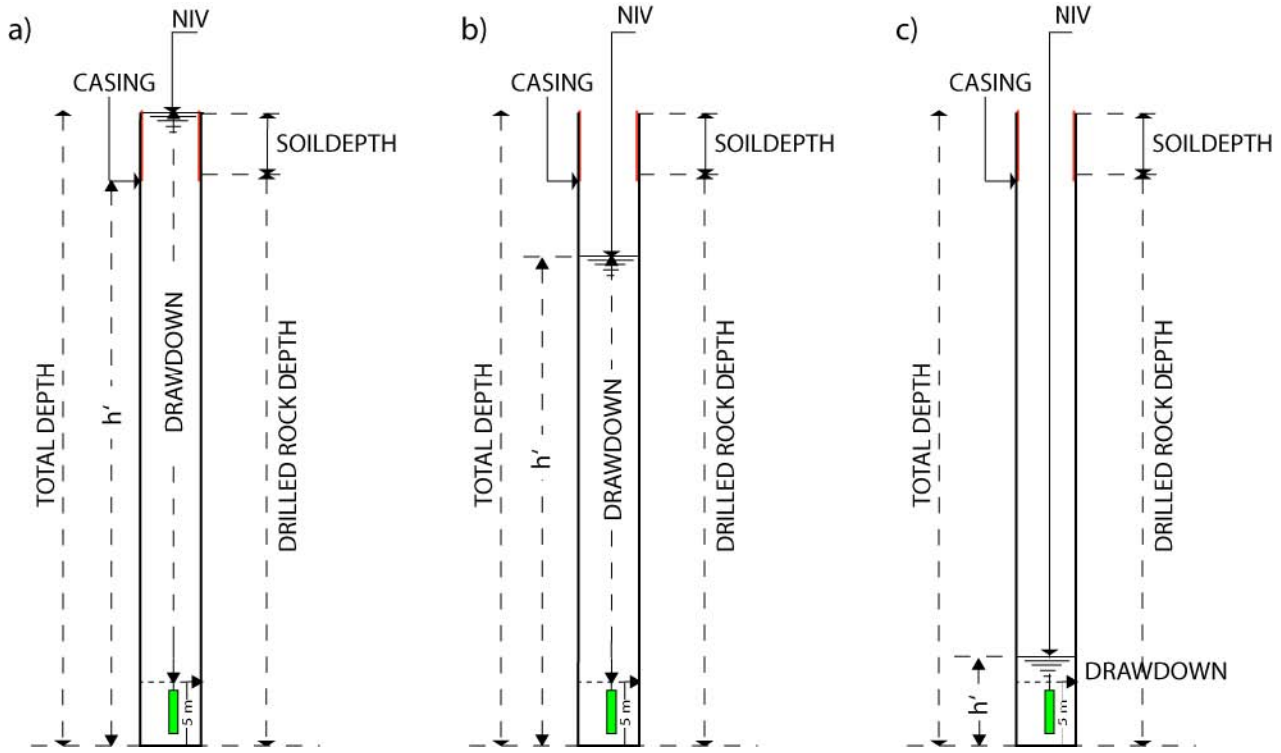

Fig. 4. Main variables used in the calculation of specific capacity and hydraulic conductivity from the borehole data with illustrations of the different situations discussed in the text.

Boreholes with missing casing data were assigned a casing depth equal to the overburden thickness plus one meter, and those with missing data about overburden thickness were assigned an overburden thickness of casing depth minus 1 meter. Borehole records with missing data about both overburden thickness and casing depths were deleted. Finally, the derived data were quality checked. Boreholes with illogical values of casing depth, the length of open section, drawdown or drilled rock depth were either reconsidered or deleted. For example a cut-off value of 60 m was set for the available drawdown, and boreholes with higher values were assigned a drawdown of 60 m.

Wells with casing lengths less than or equal to overburden thickness were excluded because the flow rates of these wells may be influenced by inflow through the overlying soils and by leakage in the transition zone between the casing and the uncased borehole. After quality-checking, the data set was reduced to about 141,400 records.

The approximations outlined above are largely the same as the ones used by Berggren (1998) and, by for example, Antal et al. (1998) in the Swedish Nuclear Fuel and Waste Management regional evaluation of hydraulic properties of the Swedish bedrock. Although the available drawdown is a conservative estimate of the drawdown, it is a better drawdown estimate than the drilled rock depth, and the approximation for specific capacity obtained by this method should be considered a better estimate of the specific capacity than the normalised well yield.

3. Geological and hydrogeological data

Geological, topographical and hydrological information were added to the technical well database by spatial joining in a GIS. This made it possible to categorise each borehole record by bedrock type, soil type, present postglacial uplift rate, relative relief and net precipitation. The different data sets and their sources are shown in Table 1.

Table 1
Characteristics of data and their sources

Type of data		Digital data characteristics	Source/details
Lithology			
	Norway	Vector data, scale 1: 3 mill	NGU (1999a)
	Sweden	Vector data, scale 1: 1 mill	SGU (1999)
Soil type			
	Norway	Vector data, scale 1:1 mill	NGU (1999b)
	Sweden	Vector data, scale 1:1mill	SGU (2001)
Present postglacial rebound rate (mm/year)		5 x 5km grid data	Dehls et al. (2000)
Runoff /net precipitation			
	Norway	1x1km grid data	Beldring et al. (2002,2003)
	Sweden	25x25 km grid data	Brandt et al. (1994), SMHI (2005)
Topography		957x957 m DEM (GTOPO)	USGS (2006)

Net precipitation is the difference between gross precipitation and evapotranspiration. It represents the potential recharge, which is the maximum theoretical amount of water available for groundwater recharge. Hence, variations in net precipitation may influence the measured flow rates of the crystalline rock boreholes. Over a long period of time, or when the system is at steady state, net precipitation equals runoff (Beldring et al., 2002; Knutsson and Morfeldt, 2002). Because runoff data are more readily available, runoff (mm/year) was taken as a surrogate parameter for potential recharge in this work (e.g. Holmén et al., 2003) and grouped into seven levels. The digital runoff maps are produced using the Nordic HBV-model (Bergström, 1995; Sælthun 1996). The level of uncertainty in the Norwegian runoff data is ± 5 -20 % (Beldring et al., 2002) and ± 10 % for the Swedish data (Brandt et al., 1994).

Topographic relief influences recharge conditions (e.g. Cherkauer and Ansari, 2005). A relative relief map was constructed from the public domain GTOPO30 digital elevation model, which has a spatial resolution of ca. 1 x 1 km, by calculating the range of elevation values in a 3 x 3 cell neighbourhood of each grid cell.

Based on their supposed hydrogeological properties, rock type was classified into five groups and soil type was classified into six groups. Readers are referred to Henriksen (2003) for details concerning this classification. The various geological, topographical and hydrological data are extracted from regional databases of small resolution rather than representing the measured quantity or property in place. For example, net precipitation at a specific site is a value indicating the potential groundwater recharge in an area that in most cases is larger than the catchment of the well.

Uplift rate and net precipitation, and to some extent also relative relief, are regional factors. Soil type, soil thickness and bedrock type represent sub-regional and local factors that may vary within the catchment of each well. From larger scale analyses, with higher data resolution, lineament neighbourhood and local topographic setting exerts an important influence on the observed flow rates (Lie and Gudmundsson, 2002; Henriksen, 2006).

4. Statistical approach and analysis

The variables in the data set are a mixture of quantitative and qualitative variables. Some of the quantitative variables are strongly skewed and are not normally distributed. Logarithmic transformation of the data results in roughly normally distributed variables and residuals respectively. Regression analyses and moving average plots were made by the computer software STATISTICA (Statsoft, 2004).

In order to explore the importance of all factors on hydraulic conductivity in the same statistical setting, the quantitative variables were classified into groups by the Jenk's optimisation method. This method groups the data into classes by identifying natural breaks in the data (Jenks, 1967; Slocum, 1999). The classified quantitative and the qualitative variables were then analysed by one-way ANOVA techniques. The results in Table 2 indicate that the variability in hydraulic conductivity and flow-rate values is best explained by the drilled rock depth, followed by uplift rate. Soil thickness, soil type and rock type have all about equal, but less importance than uplift rate. These results comply well with the results obtained from the analyses of the much smaller data sets of Henriksen (2003) and to the analyses of Berggren (1998).

Table 2
Predictor variables used in the one-way ANOVA with main results

Predictors	log Q		log K	
	R^2	F	R^2	F
Well diameter	0.026	705	0.017	450
Well use	0.029	547	0.018	324
Year drilled	0.009	283	0.029	903
Depth to static water level	0.006	187	0.008	236
Drilled rock depth	0.089	3025	0.44	24529
Soil thickness	0.039	1251	0.028	898
Soil type	0.043	1105	0.032	834
Rock type	0.039	1012	0.049	1288
Uplift rate	0.073	991	0.055	728
Runoff	0.012	397	0.008	251
Relative relief	0.002	63	0.0005	17.8

A complete assessment of log *K* and log *Q* on the predictor variables by parametric methods was done by restricting the data analysis to only one state of the qualitative variables; e.g. rock type = quartzofeldspathic rocks and soil type = absent/ thin till. Energy wells were also excluded because data from these, deeper drilled wells, may lead to underestimates of the calculated hydraulic conductivity values. The bivariate correlation matrix is shown in Table 3a. The strong correlation between log *K* and log Q ($r = 0.89$) suggests that any of the two variables could be used as indicators of hydraulic bedrock properties. However, because the drilled rock depth has a strong influence on the computation of the hydraulic conductivity, and well depth in many cases is determined by human factors, the correlations with hydraulic conductivity are likely to be more biased than the correlations with flow rate.

The predictor variables are in most cases only weakly correlated. Exceptions are well diameter and year of drilling ($r = 0.39$), and net precipitation and relative relief ($r = 0.42$). The strong correlation ($r = - 0.97$) between uplift rate and distance to the uplift centre (DISTUP) suggests that any of these two variables would serve as an indicator of the amount of isostatic uplift (e.g. Henriksen, 2003). However, because of possible irregularities in the uplift due to differential rebound, measured uplift rate with a resolution of 0.5 mm was preferred.

Table 3a
Correlation matrix between the dependent (log *K* and log *Q*) and the independent variables

	Log *K*	Log *Q*	WDIAM	DRY	DTOW	Log SOT	DRD	UPLIFT	DISTUP	NETPRE	Log RELIEF
Log *K*	1.00	0.89	- 0.03	- 0.10	- 0.02	0.10	- 0.64	- 0.08	0.08	0.04	0.03
Log *Q*	0.89	1.00	0.03	- 0.00	- 0.03	0.12	- 0.28	- 0.16	0.16	0.08	0.10
WDIAM	- 0.03	0.03	1.00	0.39	0.02	0.01	0.11	- 0.03	0.02	- 0.08	0.04
DRY	- 0.10	- 0.00	0.39	1.00	- 0.00	- 0.09	0.18	- 0.03	0.04	0.10	0.06
DTOW	- 0.02	- 0.03	0.02	- 0.00	1.00	- 0.03	0.12	- 0.02	0.02	0.05	0.12
Log SOT	0.10	0.12	0.01	- 0.09	- 0.03	1.00	- 0.08	0.01	- 0.02	0.01	0.16
DRD	- 0.64	- 0.28	0.11	0.18	0.12	- 0.08	1.00	- 0.10	0.10	0.04	0.10
UPLIFT	- 0.08	- 0.16	- 0.03	- 0.03	- 0.02	0.01	- 0.10	1.00	- 0.97	- 0.43	- 0.28
DISTUP	0.08	0.16	0.02	0.04	0.02	- 0.02	0.10	- 0.97	1.00	0.47	0.28
NETPRE	0.04	0.08	- 0.08	0.10	0.05	0.01	0.04	- 0.43	0.47	1.00	0.42
LogRELIEF	0.03	0.10	0.04	0.06	0.12	0.16	0.10	- 0.28	0.28	0.42	1.00

The tabled correlation coefficients, mostly $|r| < 0.3$, do not indicate that any of the independent variables can be considered as reliable predictors of hydraulic conductivity. For the whole data set, there is a weak negative correlation (r = - 0.08) between log *K* and uplift rate, and a correspondingly positive correlation of similar magnitude (r = 0.08) between log *K* and distance to the uplift centre. The strongest

Table 3b
Correlations between the independent variables and each of the dependent variables corrected for intercorrelations between the independent variables (partial correlations)

	WDIAM	DRY	DTOW	Log SOT	DRD	UPLIFT	NETPRE	Log RELIEF
Log *K*	0.05	0.00	0.07	0.06	- 0.65	- 0.15	- 0.01	0.06
Log *Q*	0.04	0.03	0.00	0.09	- 0.30	- 0.16	- 0.01	0.06

correlation is between log *K* and drilled rock depth (r = - 0.64). For log *Q*, these correlations are - 0.16, 0.16 and - 0.28. The weaker correlation between log *Q* and drilled rock depth illustrates the self-induced correlation in the computation of the hydraulic conductivity by formulas 2 and 3 (p. 6). Table 3b shows the bivariate correlations between each of the dependent and the independent variables after correcting for the intercorrelation effects between the independent variables.

A forward stepwise multiple linear regression gives a complete picture of the dependence of the response variable (log *K* or log *Q*) on the predictor variables individually, and at the final step of the regression it gives the bulk dependence of the response variable on the predictor variables considered. The independent variables are entered into the regression equation in a sequential manner according to their power on the explanation of the multiple correlation coefficients (Table 3b). For the whole data set, but with only wells in quartzofeldpathic rocks and with no/thin overburden or till as overburden considered, the coefficients of multiple determination (R^2) are small, and the regression model with drilled rock depth and uplift rate explains not more than about 17.1 % of the variance in log *Q*. With log *K* as the dependent variable, the same regression model explains 43.3 % of the variation.

In a study of a much smaller data set, Henriksen (2003) found different correlation between estimates of transmissivity and uplift rate in different profiles parallel to the gradients of uplift rate (Fig. 5). Table 4 summarises the results of the stepwise regression of log *Q* on the most important predictor variables in these profiles. The standardized regression coefficients (Z-coefficients in Table 4) are comparable across a common scale, and their magnitudes are indicators of the relative contribution of each predictor variable in the overall prediction of the dependent variable. Drilled rock depth is the predictor variable that contributes most, and is two to three times more important than the next important predictors except in the W-E profile 1. Here, uplift rate is the most important predictor for flow rate, followed by drilled rock depth. These relations indicate a more complex association between bedrock hydromechanical properties and uplift than that proposed by Rohr-Torp (1994) and Morland (1997).

Table 4
Summary of stepwise multiple regression
of log Q on the most important predictor variables
in profiles 1-3 from the data of Henriksen (2003).

Profile 1
log Q = 3.02 + 0.31 log UPLIFT ÷ 0.36 log DRD
(r = 0.285, R^2 = 0.081)
$Z_{\log Q}$ = 0.27$Z_{\log UPLIFT}$ ÷ 0.16$Z_{\log DRD}$

Profile 2
log Q = 1.57 ÷ 0.45 log DRD + 0.70 log PRECIP
(r = 0.206, R^2 = 0.04)
$Z_{\log Q}$ = ÷ 0.20$Z_{\log DRD}$ + 0.098$Z_{\log PRECIP}$

Profile 3
log Q = 4.03 – 0.60 log DRD – 0.14 log UPLIFT + 0.07 log SOT
(r = 0.284, R^2 = 0.081)
$Z_{\log Q}$ = ÷ 0.26$Z_{\log DRD}$ ÷ 0.09$Z_{\log UPLIFT}$ + 0.06$Z_{\log SOT}$

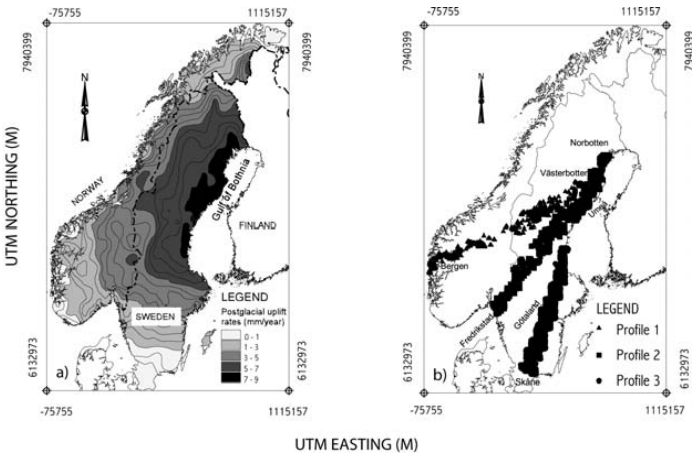

Fig.5. Maps showing the location of profiles 1-3 of Henriksen (2003)

In the present work, this suspicion is followed up by studying moving average plots of hydraulic conductivity along profiles parallel with the uplift gradients (Figs. 1 and 6). The smoothed curves, depicting the regional trends of hydraulic conductivity, are compared with profile graphs of the uplift surface in the same directions (Fig. 7).

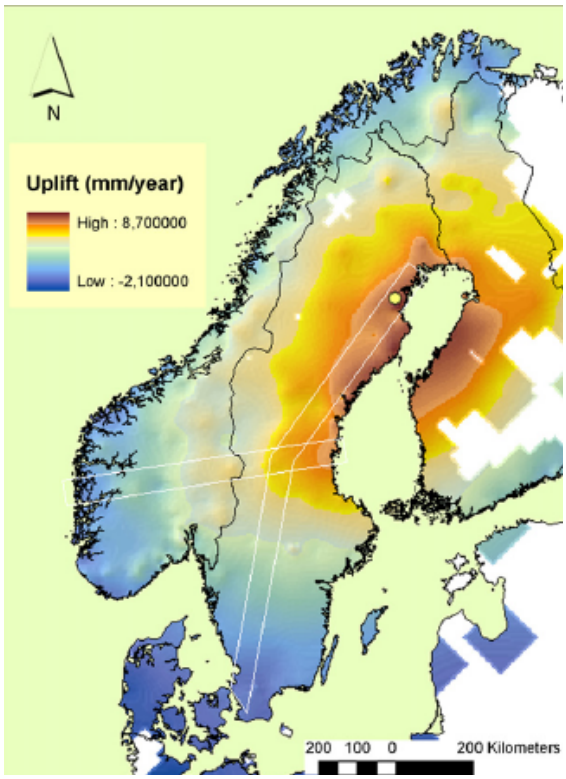

Fig. 6. Shaded relief map of the uplift surface based on the data of Dehls et al. (2000). The corridors outlined in white are parallel with the uplift gradients and contain the subsets of borehole data analysed together with the profile graphs of the uplift surface in Fig. 7. The uplift centre is shown in yellow.

Interesting features of both curves are distinct subsidiary maxima and minima, which for the uplift curves (Fig. 7a) may represent tensional uplift domes and contractional saddles in the uplift surface. Because hydraulic conductivity is a material parameter that is strongly positively correlated with fracture width, the subsidiary maxima and minima in Fig. 7 b mirror regions of, respectively, crustal tension (high K-values) and contraction (low K-values). There is a general spatial coincidence between

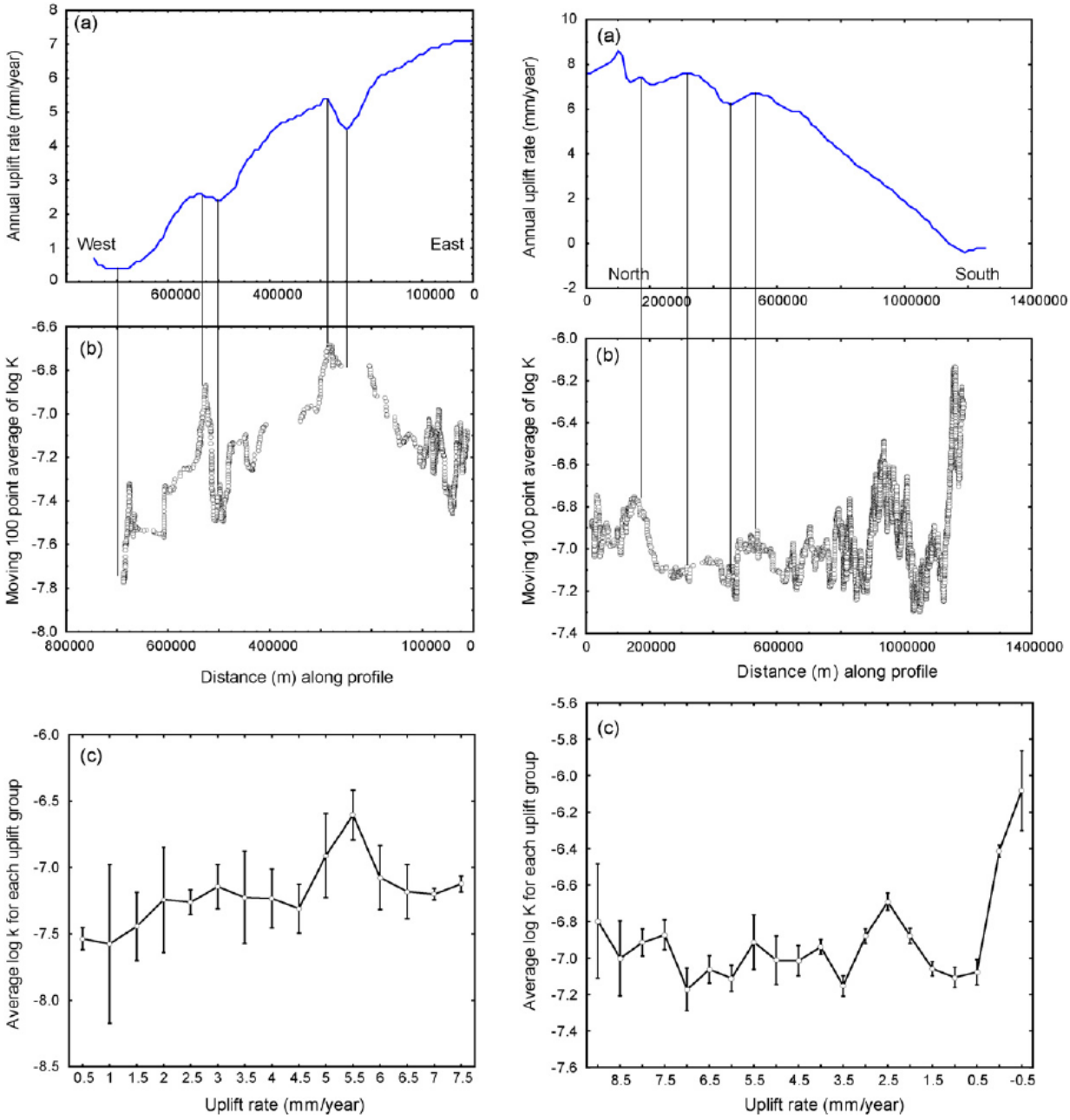

Fig.7. Profile graphs of the uplift surface in Fig. 6 (a) together with 100 points moving average plots of log *K* (b), and average log *K* values for each uplift group (c). Vertical lines connect subsidiary maxima and minima in the curves depicting uplift rate and hydraulic conductivity. Vertical bars in the bottom figures denote 0.95 confidence intervals for the mean.

subsidiary maxima or minima in the two curves, supporting the hypothesis that subsidiary minima in the uplift curve are associated with low *K*-regions, while subsidiary maxima in the uplift curve are associated with high-*K* regions. An exception is the south-central part of the N-S profile, which does not show any corresponding changes in the uplift curve. Changes in uplift gradients are also clearly depicted from the two profile graphs of the uplift surface. Similar correlations result if flow rate is used instead of hydraulic conductivity.

The traditional central-domed, thick, ice model of the Late Weichselian ice sheet was already challenged by Nesje and Dahl (1992), who suggested a multi-domed and asymmetric thin ice sheet with

a considerable variation in thickness. One likely consequence of the downmelting of such an ice sheet is a non-uniform uplift. In Fig. 6, numerous domes and basins in the uplift surface indeed indicate a highly irregular uplift pattern. With this background and also taking into account the interference with a possible Neogene tectonic uplift component (e. g. Fjeldskaar et al., 2000; Gabrielsen et al., 2005), the distribution and magnitude of late- and postglacial rebound stresses could be more complex than previously thought. The dependence of groundwater flow in fractured crystalline rocks on the contemporary stresses (e.g. Henriksen and Braathen, 2006) offers an explanation for the great variability in hydraulic conductivity along the two profiles.

5. Discussion

Of the independent predictor variables considered, all have a moderate to weak correlation with the estimates of borehole flow rate and hydraulic conductivity. Drilled rock depth stands out as the most important factor, followed by uplift rate and soil thickness.

The negative association between flow rate and drilled rock depth can be explained by several factors. It may reflect an over all decrease in permeability with depth. Increasing overburden pressure with depth will tend to close existing fractures and explains the decrease in hydraulic conductivity and well yield with depth. Relaxation joints, developed after the last glaciation, are restricted to the upper parts of the bedrock thereby influencing the vertical distribution of hydraulic conductivity and well yield. Based on model calculations, it has also been suggested that hydrofractures and shear fractures may develop at shallow depths in even massive hard rocks due to the load of the last ice sheet (Boulton et al., 1999). In a current stress field, existing fractures are also more easily reactivated at shallow depths (Alaniz-Álvarez et al., 1999; 2000), and critically stressed faults or fractures at such depths may represent structures with enhanced permeability (Barton et al., 1995; Rogers, 2003). Finally, the upper portion of the bedrock is in a more weathered state, which will also influence flow rates in a positive direction.

But the interpretation of the negative association between flow rate and drilled rock depth is difficult because the strength of the association is also influenced by non-geological factors. Most of the domestic wells are only drilled as deep as is necessary to obtain sufficient yield for the user. Shallow wells will tend to have higher flow rates compared with deeper wells, the latter being drilled to greater depths only because major water strikes were not encountered at shallower depths. Most deep wells would either have low flow rates or be failures. This results also in an overall negative association between well yield and drilled rock depth. As one likely consequence, one would expect to find the deepest wells in the less conductive parts of the bedrock and vice versa. However, only a small portion of the observed fractures in the upper crust are water conducting (Olsson et al. 1989), and even though fracture frequencies often decrease with depth, there may be no systematic decrease in permeability with depth (e.g. Loiselle and Evans, 1995; Singhal and Gupta, 1999). Zones with high hydraulic conductivity are not uncommon at depths below 150 m (e.g. Carlsson and Olsson, 1979; Daniel, 1989).

Moreover, the water conducting properties of the uppermost crust are only fully explored down to depths between 50 and 100 m because the efforts to withdraw water are minimized for most wells in the well archives. Hence, any assessments about hydraulic conductivity in the uppermost crust based on spatial variation in drilled rock depth should be treated with caution.

In an earlier analysis, based on parametric-and nonparametric one-way analysis of variance procedures (Henriksen, 2003), it was concluded that a classification based on uplift rate and precipitation did not explain more than 11% of the total regional variation in normalised flow rate along profiles parallel to the gradient of annual uplift rates. In this data set, hydraulic conductivity and flow rate shows a weak to moderate positive correlation with uplift rate along the W-E profile parallel to the

gradient of regional uplift, and a weak to moderate negative correlation along the N-S profile; which is also parallel to the gradient of regional postglacial uplift. All these results are at variance with the ideas of Rohr-Torp (1994) and Morland (1997), who found a strong positive linear correlation (*r* –values ca. 0.70 - 0.95) between uplift rate and normalised flow rate and a strong negative correlation of similar magnitude between flow rate and drilled rock depth. The correlations were interpreted in terms of a rebound related tensile-stress gradient causing gradually increased hydraulic conductivities towards the region of the greatest uplift. These analyses considered only boreholes in Norway, where present uplift rates do not exceed 5-6 mm/year. By contrast, the analyses in this work comprise solid rock boreholes from a wider region of postglacial uplift and cover the entire range of uplift rates. Here, the correlation between uplift rate and flow rate is poor (Tables 3a and 3b), and the correlation between drilled rock depth and flow rate is poorer. In Fig. 8 the relationships between the three variables flow rate, drilled rock depth and postglacial uplift rate are visualised in a 3D distance-weighted least squares surface plot

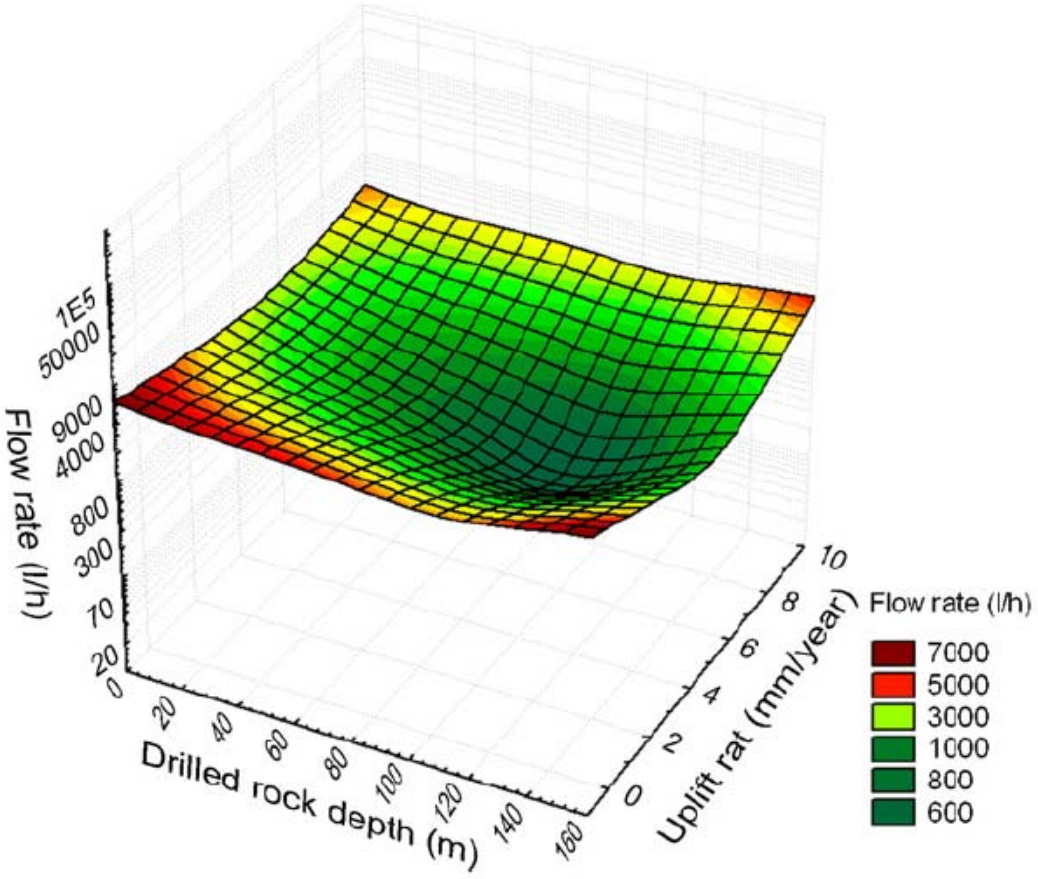

Fig. 8. The relationships among the three variables flow rate, drilled rock depth and uplift rate displayed as a smoothed 3D distance-weighted least squares surface plot of the data set of ca. 141, 000 wells.

of the data set of ca. 141, 000 wells from SW Fennoscandia. There is no unique spatial coincidence between high uplift rates and elevated flow rates/shallow well depths as would be expected if a uniform uplift was the only explanation for the variation in hydraulic conductivity. For example, high flow rates are associated with low uplift rates and shallow wells, but also with low uplift rates and deep wells and

with high uplift rates and deep wells. The significance of the minima for uplift rates between 4-5 mm/year is at present not known.

The results from this present work are in more accordance with a geostatistical analysis based on the entire well archive at the Swedish Geological Survey (Berggren, 1998), which shows no clear regional trend for the estimated permeability/hydraulic conductivity values of the bedrock in Sweden.

The uplift profiles in Fig. 7, derived from the data of Dehls et al. (2000), indicate considerable variations in uplift gradients and also differential uplift. It follows from simple models of bending of elastic plates that the flexural stresses in the concave parts of the uplift surface will be tensile down to a neutral surface at a given depth, while the stresses in the convex parts will be contractional (e.g. Turcotte and Schubert, 2002). Hence, from a hydrogeological point of view, the concave regions of gradient change should coincide with regions of higher hydraulic conductivity in contrast with the convex regions which would suffer compressive stresses and have lower *K*-values. An inspection of the couple of Fig. 7a and b is in over all agreement with this hypothesis. The strongest correlation between concave uplift regions and high hydraulic conductivity is in the W-E profile (Fig.7, left). Muir-Wood (1993a), from the analysis of geodetic leveling lines across Fennoscandia, recognised linear belts with positive and negative deviations from the regional gradient of uplift which were considered as zones of extensional and contractional deformation. However, little is presently known about the physical nature of these zones, and they could also represent shear zones developed along older faults or mega-shears (e.g. Stephansson, 1978; Talbot, 1992). The findings in this work point to a link between such zones and the hydromechanical properties of the rock mass. The lack of correlation in the south-central part of the N-S profile, where hydraulic conductivity (Fig. 7b) exhibits a considerable variability, remains at present an unexplained question. One possible explanation is that this area, i.e. the central-eastern part of Sweden, is characterised by a high density of late-and postglacial seismotectonic ground deformation features including small scale faults and fissures, bedrock-caves and pop-up blocks (e.g. Mörner et al., 1989; Mörner, 2004). In such complex structural settings, both tensional and compressional structures are likely to co-exist (e.g. Stewart and Hancock, 1994), accounting for the greater variability in hydraulic conductivity. The robustness of the proposed correlation between the second-order variations (0.2-1.2 mm) in uplift rate shown in Fig. 7 and the hydraulic data depends strongly on the resolution and accuracy of the uplift data. The uplift model used in this work relies on several sources, of which precise geodetic levellings are the most important. Lidberg et al. (2007) compared the vertical GPS-derived uplift rates from the extended BIFROST network with uplift rates from classical geodetic methods and found a very good agreement between the two approaches; i.e. a bias of 0.1 mm/year and a standard deviation of 0.5 mm/year. Mäkinen et al. (2003) also found a good agreement between GPS and leveling rates, with an rms difference of only 0.6 mm/year. Vestøl (2006) determined uplift rates calculated from leveling, tide-gauges and continuous GPS stations. The estimated reliability of this combined uplift was better than 0.4 mm/year and it was concluded that in combined uplift models the different types of data mutually control each other and increase model reliability. Compared with uplift models derived from GPS networks, the combined uplift model in this study is based on a much larger number (491) of uplift data evenly distributed across the Fennoscandian region. This improves the over all resolution of the resulting maps and contributes to a more realistic picture of the uplift than the first-order smoothed oval-shaped contours, compatible with an unbroken uniform uplift, that are often shown. In light of this, and also bearing in mind other evidence/indications of late- and postglacial differential movements, it cannot be excluded that the second-order features in Fig. 7a reflect vertical movement zones between blocks undergoing differential uplift.

That the true uplift experienced by Fennoscandia is more complicated than that of a passive uniform uplift is evident from a number of reported disturbances in uplift rates from local and regional studies based on shore lines, geodetic levellings and GPS campaigns (e.g. Mörner, 1979; Björkman and Trägårdh, 1982; Anundsen, 1989; Talbot, 1992; Tirén and Beckholmen, 1992; Påsse, 2001; Risberg et al., 2005). Rock-block models for the glacio-isostatic recovery in Fennoscandia were proposed by Påsse

(2001) and Olesen et al. (2004). In these models, the glacio-isostatic adjustments are depicted as subsidence and uplift of rigid crustal blocks along narrow zones rather than being a uniform doming process. Spatial correlation between zones of recent differential uplift and fracturing is also described from western Switzerland by Jaboyedoff et al. (2003).

It is also clear that the stresses and strain fields associated with the glacial loading and unloading are neither uniformly distributed nor symmetrically related to the uplift centre. Analyses of Global Positioning System (GPS) data in the BIFROST network (Milne et al., 2001) demonstrate an ongoing horizontal extensional deformation of the Fennoscandian crust due to the glacial uplift. However, the observed and predicted deformation rates are not symmetrically distributed about the region of maximum uplift. The highest deformation rates are westward and northward from the centre of uplift. And although the horizontal strains tend to radiate outward from this region, they increase with distance from the centre of uplift.

Although recognised as a significant factor, uplift-generated stresses caused by the removal of the Late Weichselian ice sheet is only one of several factors that affect flow rates of the hard rock boreholes in this area. Other current and competing stress field such as ridge push stresses from the mid – Atlantic ridge and sedimentary loading stresses (Fejerskov and Lindholm, 2000) will interact with the rebound stresses to affect fracture apertures and hydraulic properties of the rock mass at any site. Subregional and local factors, such as topography, in-situ rock stresses and distances to lineaments will also influence the flow rates at a particular site (Brook, 1988; Henriksen, 1995; Caine et al., 1996; Miller and Dunne, 1996; Morin and Savage, 2002; Henriksen and Braathen, 2006). However, the inclusion and evaluation of these factors in a regional statistical setting requires, for example, high precision lineament data for the whole study area. Such data are currently not available.

6. Conclusions

Of the variables evaluated in this study, drilled rock depth and observed present rate of uplift stand out as the most important predictor for flow rate and hydraulic conductivity in the uppermost crust of Fennoscandia. The two factors are wholly or in part related to late Quaternary rebound of the downwarped Fennoscandian crust. Drilled rock depth has a potential human bias, but its significance can also be explained geologically. It is typically two or three times as important predictor as uplift rate, but in a W-E profile uplift rate is nearly twice as important predictor than drilled rock depth. The other variables are either poor or not significant predictor variables in the regression models.

Uplift rate is also recognised as an important predictor variable for hydromechanical bedrock properties. The altogether poor predictive power of the regression models and the fact that different profiles along the uplift gradients give different models suggest that other factors are better predictors for flow rates and hydraulic properties of the rock mass. Nevertheless it is considered that late- and postglacial rebound plays an important role in explaining the variation in hydromechanical properties of the crystalline rocks. However, hydraulic conductivity of the upper crust does not vary in a systematic manner along the uplift gradients. It is only poorly correlated with uplift rates directly, but rather with linear belts where uplift rates are abruptly changing and where stress concentrations cause detectable variations in the estimates of the hydraulic conductivity. If this assertion is valid, it follows that the synoptic analysis of hydraulic conductivity with profile graphs of uplift rate may contribute to the understanding of the geodynamics associated with the late glacial and Holocene deglaciation. These findings suggest that the rebound tectonics are difficult to interpret as an unbroken and uniform uplift of a downwarped crust.

Acknowledgements

Agust Gudmundsson and Atle Nesje made comments on an early version of the manuscript. Reviews by Willy Fjeldskaar and an anonymous referee provided constructive comments that improved the manuscript. John Dehls provided background material for the Neotectonic map of Norway and adjacent areas. All these contributions are gratefully acknowledged.

References

Alaniz-Álvarez, S.A., Tolson, G., Nieto-Amaniego, Á. F., 1999. A graphical technique to predict slip along a pre-existing plane of weakness. Engineering Geology 49, p. 53-60.

Alaniz-Álvarez, S.A., Tolson, G., Nieto-Amaniego, Á. F., 2000. Assessing Fault Reactivation with the Reactiva program. Journal of Geoscience Education 48, p. 651-657.

Andersen, B.G., 1981. Late Weichselian ice sheets in Eurasia and Greenland. In: Denton, G.H., Hughes, T.J. (Eds.), The Last Great Ice Sheets. John Wiley, New York, pp. 1-65.

Antal I., Bergman T., Gierup J., Persson M, Thunholm B., Wahlgren C-H., Stephens M., Johansson R., 1998. Översiktsstudie av Blekinge län. Geologiska förutsättningar. SKB Report R-98-22.

Anundsen, K,. 1989. Late Weichselian relative sea levels in southwest Norway: observed strandline tilts and neotectonic activity. Geologiska Föreningens i Stockholm Förhandlingar 111, 288-292.

Babuska V., Plomerova J., Pajdusak P., 1988. Seismologically determined deep lithosphere structure in Fennoscandia. Geologiska Föreningen i Stockholms Förhandlingar 111, 288-292.

Barton, C.A., Zoback, M.D., Moos, D., 1995. Fluid flow along potentially active faults in crystalline rock. Geology 23 no.8, 683-686.

Beldring, S., Roald, L.A:, Voksø, A., 2002. Avrenningskart for Norge. Årsmiddelverdier for avrenning 1961-1990. NVE-report 2, 2002,(Runoff map of Norway. Yearly runoff-means 1961-1990. The Norwegian Water Resources and Energy Directorate report 2, 2002)

Beldring, S., Engeland, K., Roald, LA, Sælthun NR, Voksø A., 2003. Estimation of parameters in a distributed precipitation-runoff modell for Norway. Hydrology and Earth System Sciences 7, 304-316.

Berggren, M., 1998. Hydraulic conductivity in Swedish bedrock estimated by means of geostatistics: Thesis report series 1988:9, Royal Institute of Technology (KTH), Department of Civil and Environmental Engineering, Division of Land and Water Resources, Stockholm, Sweden.

Bergström, S., 1995. The HBVmodel. In: Sing,V.P. (Ed.), Computer Models of Watershed Hydrology, 443-476. Water Resources Publications, Highlands Ranch.

Björkman H, Trägårdh J., 1982. Differential uplift in Blekinge indicating late-glacial tectonics. Geologiska Föreningens i Stockholm Förhandlingar 104, 75-79.

Boulton, G.S., Caban, P. Hulton, N., 1999. Simulations of the Scandinavian ice sheet and its subsurface conditions. Swedish Nuclear Fuel and Waste Management Co. (SKB) Report R-99-73, Stockholm.

Brandt, M., Jutman, T., Alexandersson, H., 1994. Sveriges vattenbalans. Årsmedelvärden 1961-1990 av nederbörd, avdunstning och avrinning, SMHI Hydrologi Nr. 49, 16 s. (The Water Balance of Sweden. Yearly precipitation, evaporation and runoff means 1961-1990. SMHI hydrologi 49, 16 pp).

Brook, G.A., 1988. Hydrogeological factors influencing well productivity in the crystalline rocks of Georgia. South Eastern Geology 29, 65–81.

Caine, S.C., Evans, J.P., Forster, C.B., 1996. Fault zone archietecture and permeability structure. Geology 24, no.11, 1025-1028.

Carlsson, L., Carlstedt, A., 1977. Estimation of Transmissivity and permeability in Swedish Bedrock. Nordic Hydrology 8, 103-116.

Carlsson, A., Olsson, T. 1979. Ground water in Swedish hard-rock areas- a multiple aquifer system. Symposium on Methods for Evaluation of Ground-water Resources. Vilnius. 99-102

Cherkauer, D.S., Ansari S.A. 2005: Estimating Ground Water Recharge from Topography, Hydrogeology, and Land Cover. Ground Water 43, 102-112

Cohen, A.J.B., 1995. Hydrogeologic Characterization of Fractured Rock Formations: A Guide for Groundwater Remediators. Report LBL38142, Earth Sciences Division Ernest, Orlando Lawrence Berkeley National Laboratory Berkeley Lab. University of California, Berkeley USA.

Daniel III, C.C., 1989. Statistical analysis relating well yield to construction practices and siting of wells in the Piedmont and Blue Ridge Provinces of North Carolina. U.S. Geological Survey Water-Supply Paper 2341-A, 27 pp.

Dehls, J.F., Olesen, O., Bungum, H., Hicks, E.C., Lindholm, C.D., Riis, F., 2000. Neotectonic map: Norway and adjacent areas, 1:3 000 000. Geological Survey of Norway, Trondheim.

Ekman, M., 1991. Course and origin of the Fennoscandian uplift: the case for two separate mechanisms. Terra Nova 3, 408 – 413.

Ekman, M., 1996. A consistent map of the postglacial uplift of Fennoscandia: Terra Nova 8, 158-165.

Erlström, M., Thomas, S.A., Deeks, N., Sivhed, U., 1997. Structure and tectonic evolution of the Tornquist Zone and adjacent sedimentary basins in Scania and the southern Baltic Sea area. Tectonophysics 271, 191-215

Faleide, J.I., Kyrkjebø, R., Kjennerud, T., Gabrielsen, R.H., Jordt, H., Fanavoll, S., Bjerk, M.D., 2002. Tectonic impact on sedimentary processes during Cenozoic evolution of the northern North Sea and surrounding areas. In: Dore´, A.G., Cartwright, J.A., Stoker, M.S., Turner,

J.P. & White, N.J. (Eds.), Exhumation of the North Atlantic Margin; Timing, Mechanisms and Implications for Petroleum Exploration. Geological Society, London, Special Publications, 196, 235–269.

Fejerskov, M., and Lindholm, C., 2000, Crustal stresses in and around Norway: an evaluation of stress generating mechanisms. In: Nöttvedt and others (Eds.), Dynamics of the Norwegian Margin. Geological Society London, Special Publication 107, pp. 451-467.

Fjeldskaar, W.; Cathles, L. 1991: The present rate of uplift of Fennoscandia implies a low-viscosity asthenoshere. Terra Nova 3, 393- 400.

Fjeldskaar, W., Lindholm, C., Dehls, J.F., Fjeldskaar, I., 2000. Postglacial uplift, neotectonics and seismicity in Fennoscandia. Quaternary Science Reviews 19, 1413-1422.

Gabrielsen, R.H., Braathen, A., Olesen, O., Faleide, J.I., Kyrkjebø, R., Redfield, T.F., 2005. Vertical movements in south-western Fennoscandia: a discussion of regions and processes from the Present to the Devonian. In: Wandas, B.T.G., Nystuen, J.P., Eide, E.A. & Gradstein, F.M. (Eds.) Onshore-Offshore Relationships on the North Atlantic Margin. Norwegian Petroleum Society (NPF) Special Publications, 12, pp. 1-28.

Gudmundsson, A., 1999. Postglacial crustal doming, stresses and fracture formation with application to Norway: Tectonophysics 307, p. 407-419.

Henriksen, H., 1995. Relation between Topography and Borehole Yield in Boreholes in Crystalline Rocks, Sogn og Fjordane, Norway: Ground Water 33, 635-643.
Henriksen, H., 2003. The role of some regional factors in the assessment of well yields from hard-rock aquifers of Fennoscandia: Hydrogeology Journal v.11, 628 - 645.
Henriksen, H., Braathen, A., 2006. Effects of fracture-lineaments and in situ rock stresses on groundwater flow in hard rock: A case study from Sunnfjord, Western Norway. Hydrogeology Journal 14, 444 - 461.
Henriksen, H., 2006. Fracture lineaments and their surroundings with respect to groundwater flow in the hard rocks of Sunnfjord, western Norway. Norwegian Journal of Geology (in review)
Holmén GH, Stigsson M., Marsic M, Gylling B., 2003. Modelling of groundwater flow and flow paths for a large regional domain in northeast Uppland. SKB (Swedish Nuclear Fuel and Waste Management CO) Report R-03-24, 162 pp.
Jaboyedoff, M., Baillifard, F., Derron, M-C. 2003: Preliminary note on uplift rate gradients, seismic activity and possible implications for brittle tectonics and rockslide prone areas: The example of western Switzerland. Bull. Soc. Vaud. Sc.Nat. 88, 401-420.
Jenks, G.F., 1967. The Data Model Concept in Statistical Mapping, International Yearbook of Cartography 7, 186-190.
Jetel, J., 1964. Pouzití hodno specifické-vydatnostia novycg odvozenych parametrúv hydrogeologií. Geol. pruzk 6, 144-145. Praha.
Jetel, J., Krásný, J., 1968. Approximative aquifer characteristics in regional hydrogeological study. Vest.Ustr. geol., 43, 459-461. Praha.
Kaufmann, G.; Wu, P., Guoying, L., 2000. Glacial isostatic adjustment in Fennoscandia for a laterally homogeneous earth. Geophys. J. Int. 143, 262-273.
Kinck, J.J., Husebye, E.S., Lund, C-E., 1991. The South Scandinavian crust: structural complexities from seismic reflection and refraction profiling. Tectonophysics 189, 117-133.
Knutssson, G., Morfeldt, C.O., 2002. Grundvatten. Teori & tillämpning. (Groundwater. Theory and applications). AB Svensk Byggtjänst. Stockholm, Sweden.
Krásný, J., 1999. Hard-rock hydrogeology in the Czech Republic. Hydrogéologie 2, 25-38.
Kullerud, L., Tørudbakken, B.O., Ilebekk, S., 1986. A compilation of radiometric age determinations from the Western Gneiss Region, South Norway. Geological Survey of Norway Bulletin 406, 17-42
Lambeck, K., Smither,C., Johnston, P., 1988. Sea-level change, glacial rebound and mantle viscosity for northern Europe. Geophys. J.Int. 134, 102-144.
Lidberg,M., Johansson, J.M., Scherneck, H.G., Davis, J.L., 2007. An improved and extended GPS-derived 3D velocity field of the glacial isostatic adjustment (GIA) in Fennoscandiaa. J. Geodesy 81, 213-230.
Lidmar-Bergström, K., 1999. Uplift histories revealed by landforms of the Scandinavian domes. In: Smith, B.J., Warke, P.A., (Eds) : Uplift, Erosion and Stability: Pesrpectives on Long-Term Landscape Development. Geological Society of London, Special Publication 162, 85-91.
Lie, H., Gudmundsson, A., 2002. The importance of hydraulic gradient, lineament trend, proximity to lineaments and surface drainage pattern for yield of groundwater wells on Askøy, West-Norway. Geological Survey of Norway Bulletin 439, 51-60.
Loiselle, M., Evans, D., 1995. Fracture Density Distributions and Well Yields in Coastal Maine. Ground Water 33, 190-196.
Lundqvist, J. 1996. Late Weichselian Glaciation and deglaciation in Scandinavia. Quaternary Science Reviews 5, 269-293.
Mäkinen, J., Koivukla, H., Poutaanen, M., Saaranen, V., 2003. Vertcal velocities in Finland from permanent GPS networks and from repeated precise levelling. Journal of Geoduynamics 38, 443-456.
Mangerud, J. 1991. The last ice age in Scandinavia. Striae 34, 15-30.
Milne, G.A., Davis, J.L., Mitrovica, J.X., Scherneck, H.-G., Johansson, J.M., Vermeer, M., Koivula, H. 2001. Space-Geodetic Constraints on Glacial Isostatic Adjustment In Fennoscandia. Science 291, 2381-2385.
Milne, GA, Mitrovica JX, Scherneck, H.-G., Davis JL, Johansson, J.M., Koivula, H, Vermeer M., 2004. Continuous GPS measurements of postglacial adjustment in Fennoscandia:2. Modeling results. Journal of Geophysical Research 109, B02412.
Milnes, A.G., Wennberg, O.P., Skår ,Ø., Koestler, A.G., 1997. Contraction, extension and timing in the South Norwegian Caledonides: the Sognefjord transect. In: Burg JP, Ford, M. (Eds.), 1997: Orogeny Through Time. Geological Society Special Publication 121, 123-148.
Miller, D.J., Dunne, T., 1996. Topographic perturbations of regional stresses and consequent fracturing. J. Geophys. Res. 101, 25,523-25,536.
Mitrovica, J.X, Davis, J.L, Shapiro, I.I., 1994. A spectral formalism for computing three-dimensional deformations due to surface loads 2. Present –day glacial isostatic adjustment. Journal of Geophysical Research 99 (B4), 7075-7101.
Morin, R.H., Savage, W.Z., 2002. Topographic stress perturbations in southern Davis Mountains, west Texas. 2. Hydrogeologic implications. Jour.Geophys.Res. 107, B12,ETG. 6.1-6.10.
Morland, G., 1997. Petrology, Lithology, Bedrock Structures, Glaciation and Sea Level. Important Factors for Groundwater Yield and Composition of Norwegian Bedrock Boreholes? Geological Survey of Norway Report 97.122 I.
Muir-Wood, R., 1993a. A review of the seismotectonics of Sweden. Swedish Nuclear Fuel and Waste Management Co (SKB) Technical Report 93-13, Stockholm.
Muir-Wood, R., 1993b. Hydrological signatures of earthquake strain. Journal of geophysical research 98, B12, 22035-22068.
Muir-Wood, R., 2000. Deglaciation Seismotectonics: a principal influence on intraplate seismogenesis at high latitudes. Quaternary Science Reviews 19, 1399-1411.
Mörner, N.-A., 1979. The Fennoscandian uplift and Late Cenozoic Geodynamics: Geological Evidence. GeoJournal 3, 287-318.
Mörner, N.-A., 1980. The Fennoscandian uplift: geological data and their geodynamical implication: In (Mörner, N.A ,ed.), Earth Rheology, Isostasy and Eustasy, p. 251-284. John Wiley & Sons.
Mörner, N.-A., 1985. Paleoseismicity and geodynamics in Sweden ,Tectonophysics 117, 139-153.
Mörner, N.-A., Somi, E.., Zuchiewicz, W., 1989. Neotectonics and Paleoseismicity within the Stockholm intracratonal region in Sweden. Tectonophysics 163, 289-303.
Mörner, N.-A., 2004. Active faults and paleoseismicity in Fennoscandia, especially Sweden. Primary structures and secondary effects. Tectonophysics 380, 139-157.
Nesje, A., Dahl, S.O., 1992. Geometry, thickness and isostatic loading of the Late Weichselian Scandinavian ice sheet: Norwegian Journal of Geology 72, 271-273.
NGU, 1999a. Digital Bedrock Database of Norway 1:3mill. The Geological Survey of Norway, Trondheim, Norway.
NGU, 1999b. Digital Database of Surficial Deposits of Norway, 1:1mill. The Geological Survey of Norway, Trondheim, Norway.
NRC, 1996. Rock Fractures and Fluid Flow. Contemporary Understanding and Applications. US National Research Council. National Academy Press, Washington.
Olesen, O., Dehls, J., Bungum, H., Riis, F., Hicks, E., Lindholm, C., Blikra L.H., Fjeldskaar, W., Olsen, L., Longva, O., Faleide, J.I., Bockmann, L., Rise, R., Roberts, D., Braathen A., Brekke, H.: 2000. Neotectonics in Norway, Final Report. The Geological Survey of Trondheim, Norway, Report no. 2000.002, 119 pp.
Olesen, O., Blikra. L.H., Braathen, A., Dehls, J.F., Olsen, L., Rise, R., Roberts, D., Riis, F., Faleide, J.I., Anda, E., 2004. Neotectonic deformation in Norway and its implications: a review. Norwegian Journal of Geology 84, 3-17.
Olsson, O., Black, J., Gale, J.E., Holmes, D.C. 1989: Site characterization and validation, Stage 2 Preliminary predictions. Swedish Nuclear Fuel and Waste Management Co (SKB) Technical Report 89-03, Stockholm.

Pan, M., Sjøberg, L.E., Talbot, C.J., Asenjo, E., 1999. GPS measurements of crustal deformation in Skåne, Sweden, between 1989 and 1996. Geologiska Föreningens i Stockholm Förhandlingar 121, 67-72.
Påsse, T., 2001. An empirical model of glacio-isostatic movements and shore-level displacement in Fennoscandia: Swedish Nuclear Fuel and Waste Management Co. (SKB) Report R-01-41, Stockholm.
Risberg, J., Alm, G., Goslar,T. 2005. variable isostatic uplift patterns during the Holocene in southeast Sweden, based on high-resolution AMS radiocarbon datings of lake isolations. The Holocene 15, 847-857.
Riis, F., 1996. Quantification of Cenozoic vertical movements of Scandinavia by correlation of morphological surfaces with offshore data. Global and Planetary Change 12, 331-357.
Rogers, S.F., 2003. Critical stress-related permeability in fractured rocks. In: Ameen, M. (Ed.), Fracture and In-Situ Stress Characterization of Hydrocarbon Reservoirs. Geological Society London, Special Publication 209, 7-16.
Rohr-Torp, E., 1994. Present uplift rates and groundwater potential in Norwegian hard rocks. Geological Survey of Norway Bulletin 426, 47-52.
SGU, 1999. National Bedrock Database 1:1 mill. Dnr: 00-751/99. Geological Survey of Sweden, Uppsala, Sweden.
SGU, 2001. National Database of Surficial Deposits 1:1mill. Dnr: 00-410/2001. Geological Survey of Sweden, Uppsala, Sweden.
Sigmond, E.M.O., 2002. Geologisk kart over land- og havområder i nord- Europa, 1: 4 mill. (Geological map of land- and ocean areas in northern Europe, 1:4 mill). Geological Survey of Norway.
Singhal, B.B.S., Gupta, R.P., 1999. Applied Hydrogeology of Fractured Rocks. Kluwer Academic Publishers.
Slocum, T., 1999. Thematic Cartography and Visualization. Prentice Hall 1999.
SMHI, 2005. Digital Map 1: 2, 5 mill. of mean annual runoff 1960-1991. Swedish Hydrological and Meteorological Institute, Norrköping, Sweden.
StatSoft, Inc. 2004. STATISTICA (data analysis software system), version 7. www.statsoft.com.
Stephansson, O., 1978. Seismo-tectonics in Fennoscandia. Geologiska Föreningens i Stockholm Förhandlingar 110, 239-245.
Stewart, I.S., Hancock, P.L. 1994. Neotectonics. In: Hancock, P.L. (Ed) Continental Deformation Pergamon Press, pp 370-409.
Sælthun, N.R., 1996. The Nordic HBV model. NVE (Norwegian Water Resources and Energy Administration) report 07-1996.
Talbot, C.J., 1992. GPS network to measure active strains in Sweden. Geologiska Föreningens i Stockholm Förhandlingar 114, 378-380.
Tirén S.A. , Beckholmen, M., 1989. Block faulting in southeastern Sweden interpreted from digital terrain models. Geologiska Föreningens i Stockholm Förhandlingar 111, 171-179.
Tirén, S.A., Beckholmen, M. 1992. Rock block map analysis of southern Sweden. Geologiska Föreningens i Stockholm Förhandlingar 114, 253-269.
Turcotte, D.L., Schubert, G., 2002. Geodynamics, 2nd ed. Cambridge University Press, New York.
USGS, 2006. GTOPO30 (Global 30 Arc-Second Elevation Data Set). Product description. http://edc.usgs.gov/products/elevation/gtopo30.html
Vestøl, O. 2006. Determination of Postglacial Land Uplift in Fennoscandia from Levelling, Tide-gauges and Continuous GPS Stations using Least Squares Collocation. Journal of geodesy 80, 248-258.
Wallroth, T., Rosenbaum, M.S., 1995. Estimating the spatial variability of specific capacity from a Swedish regional database. Mar. Petrol. Geol. 13, 457-461.
Wladis, D., Gustafson, G., 1999. Regional characterization of hydraulic properties of rock using air-lift data. Hydrogeology J. 7, 168-179.
Wu, P., Johnston, P., Lambeck, K., 1999. Postglacial rebound and fault instability in Fennoscandia. Geophys. J.l Int. 139, 657-670.